Secondary Structure and Oligomerization of the *E. coli* Glycerol Facilitator[†]

Darren M. Manley, Mark E. McComb, Hélène Perreault, Lynda J. Donald, Harry W. Duckworth, and Joe D. O'Neil*

Department of Chemistry, University of Manitoba, Winnipeg, Manitoba R3T 2N2, Canada

Received March 28, 2000; Revised Manuscript Received July 13, 2000

ABSTRACT: The Major Intrinsic Proteins are found throughout the bacterial, plant, and animal kingdoms and are responsible for the rapid transport of water and other small, polar solutes across membranes. The superfamily includes the aquaporins, the aquaglyceroporins, and the glycerol facilitators. We have overexpressed and purified the *Escherichia coli* inner membrane glycerol facilitator. Approximately 7.5 mg of 95% pure protein is obtained from 1 L of *Escherichia coli* cells using immobilized metal affinity chromatography. Well-resolved matrix-assisted laser desorption ionization mass spectra were obtained by solubilization of the protein in octyl-β-D-glucopyranoside (M_r = 33 650.3; error ~0.4%). The recombinant glycerol facilitator is inserted into the bacterial inner membrane, is functional, and is inhibited by $HgCl_2$. Polyacrylamide gel electrophoresis suggests that the facilitator is predominantly monomeric when solubilized with dodecyl-β-D-maltoside, octyl-β-D-glucopyranoside, and sodium dodecyl sulfate, but that it self-associates, forming soluble oligomers when urea is used during extraction. Similar oligomeric species are demonstrated to exist in the bacterial membrane by chemical cross-linking experiments. Circular dichroism analysis shows that the protein is predominantly α-helical. Helix content is significantly higher in protein prepared in the absence of urea (42−55%) than in its presence (32%). A possible role for the facilitator oligomers in interactions with, and regulation of, the glycerol kinase is discussed.

Several species of bacterium are able to utilize glycerol as their sole carbon and energy source (*1*), and it has been known for over 20 years that bacteria express specific protein pores to facilitate nonsaturable, low energy of activation (E_a = 4.5 kcal/mol) transport of glycerol across their membranes (*2*). The transport properties of the *E. coli* glycerol facilitator (GF)[1] have been measured both in the bacterium and in *Xenopus* oocytes (*2*−*6*). The protein permits passage of glycerol and other low molecular weight polyols, but not sugars. Conflicting reports have suggested that the glycerol facilitator does not transport water (*4*) and that transport is measurable but minor compared to glycerol transport (*5*). Transport by the facilitator is apparently affected by membrane lipid composition (*7*).

In mammals, glycerol transport is an essential activity in several tissues including hepatocytes and adipocytes, both of which take up glycerol released by triacylglycerol hydrolysis. Adipocytes also export glycerol following lipolysis. Candidate glycerol transporters have been identified in human adipocytes and rat spermatids (aquaporin-7) (*8*, *9*), in rat hepatocytes (aquaporin-9) (*10*), and in a variety of tissues that express aquaporin-3 (*11*). Aquaporins-3, -7, and -9 are sometimes called aquaglyceroporins, reflecting their dual specificities and their phylogenetic homology to the bacterial glycerol facilitators (*12*).

Although water crosses lipid bilayers in the absence of a pore at a surprisingly rapid rate (10 μm/s) (*13*), animals, plants, and bacteria also express membrane channels that are highly selective for water (*9*). In *E. coli*, aquaporin-Z (AQPZ) permits the cell to specifically respond to changes in the osmolality of its environment (*5*). In mammals, AQPs 0, 1, 2, 4, 5, 6, and 8 easily discriminate between water and urea, which have radii of 1.5 and 2.0 Å, respectively (*14*, *15*). Transport assays suggest that the capacity to transport water varies widely among the aquaporins; AQPs 2 and 4 are highly efficient water pores whereas AQP0 barely elevates water transport above passive diffusion in those cells in which it is expressed (*14*).

The glycerol facilitators, aquaporins, and aquaglyceroporins comprise a superfamily of proteins (*12*) named after the first discovered aquaporin, the Major Intrinsic Protein (MIP) of the eye lens fiber (see *16* and references cited within). The proteins are distinguishable by their pore specificities (*9*), amino acid sequences, and the organization of their genes (*12*). Hydropathic analysis (*17*) suggests that the protein fold contains six membrane-spanning helices (1−6) connected by five loops (A−E). Loops B and E contain a characteristic Asn-Pro-Ala motif (*18*) that is found in every member of the family and may form an important component of the channel pore. The most thoroughly characterized MIP is the

[†] The financial assistance of the Natural Sciences and Engineering Research Council and the University of Manitoba is gratefully acknowledged.

* To whom correspondence should be addressed.

[1] Abbreviations: AQP, aquaporin; DM, dodecyl-β-D-maltoside; OG, octyl-β-D-glucopyranoside; DSS, disuccinimidyl suberate; EDTA, ethylenediaminetetraacetic acid; GF, glycerol facilitator; HPLC, high-performance liquid chromatography; IPTG, isopropyl-β-D-thiogalactopyranoside; kDa, kilodalton(s); LB, Luria−Bertani; MALDI, matrix-assisted laser desorption ionization; MIP, major intrinsic protein; M_r, relative molecular mass; NTA, nitrilotriacetic acid; OD, optical density; PCR, polymerase chain reaction; PU, polyurethane; SDS−PAGE, sodium dodecyl sulfate−polyacrylamide gel electrophoresis; TB, terrific broth; TOFMS, time-of-flight mass spectrometry; Tris, tris(hydroxymethyl)aminomethane.

10.1021/bi000703t CCC: $19.00
Published on Web 09/16/2000

highly abundant red blood cell channel forming integral protein, AQP1 (*19*). The amino and carboxyl termini and loops B and D of AQP1 have been shown to reside on the cytoplasmic side of the red cell membrane (*20*), with loops A, C, and E found outside the cell (*21*). Biochemical (*20*), freeze−fracture (*22*), and electron crystallographic analyses (*23*, *24*) indicate that AQP1 is a homotetramer, with an extracellular complex glycan attached to an asparagine in one of the four subunits (*20*). Radiation inactivation (*25*) and studies with chimeric molecules (*26*) have shown that each monomer in the tetramer contains an active pore. Electron crystallographic analysis has yielded structures at approximately 6 Å resolution allowing visualization of six tilted transmembrane helices (*23*, *24*). The structures also suggest that the NPA-containing loops B and E penetrate the membrane bilayer (*27*). Several mutations within loops B and E, including the NPA residues, inactivate the pore, supporting suggestions that the loops comprise important parts of the channel wall (*27*, *28*).

Understanding the substrate specificities and transport mechanisms of the Major Intrinsic Proteins requires high-resolution structure determination of several family members with differing specificities. We have cloned, overexpressed, and purified the *E. coli* GF. Secondary structure and oligomerization of the recombinant protein were studied in four different detergent preparations and in membranes by mass spectrometry, circular dichroism, polyacrylamide gel electrophoresis, and chemical cross-linking experiments.

MATERIALS AND METHODS

Materials

Lauryldimethylamine oxide was obtained from Calbiochem (San Diego, CA). Dodecyl-β-D-maltoside was purchased from Anatrace (Maumee, OH). Sodium dodecyl sulfate, octyl-β-D-glucopyranoside, *N*-laurylsarcosine, Triton X-100, Tween 80, rifampicin, sodium deoxycholate, urea, sinapinic acid, nitro blue tetrazolium, 5-bromo-4-chloro-3-indolyl phosphate, equine heart myoglobin (16 951 Da), and bovine insulin (5733 Da) were obtained from Sigma (St. Louis, MO). DNA amplification was performed using the Expand High Fidelity PCR system, and dNTPs from Boehringer Manheim (Laval, QC), which was also the source of the 5-bromo-4-chloro-3-indolyl-β-D-galactopyranoside. PCR primers were made in the Department of Microbiology, University of Manitoba. Mutagenesis primers, restriction endonucleases, T4 DNA ligase, T4 polynucleotide kinase, and the Klenow fragment of DNA polymerase I were purchased from Life Technologies (Rockville, MD). Helper phage R408 was obtained from Promega (Madison, WI). Ready-to-go pUC18, precut at the *Sma*I site, was obtained from Pharmacia Biotech (Baie d'Urfé, QC). The pET28b-(+) expression vector, anti-T7 antibody−alkaline phosphatase conjugate, and the bacterial strains Novablue, BL21(DE3), and BL21(DE3)pLysS were obtained from Novagen (Madison, WI). Nickel nitrilotriacetic acid (NTA) resin was from Qiagen (Toronto, ON). Disuccinimidyl suberate, disuccinimidyl gluterate, and bis(sulfosuccinimidyl) suberate were purchased from Pierce (Rockford, IL). HPLC-grade acetonitrile and methanol were from Fisher Scientific (Fair Lawn, NJ). Deionized water was prepared with a Milli-Q plus-TOC water purification system (Millipore, Bedford, MA). The nonporous ether-type PU membrane, 50 μm in thickness (XPR625-FS), was supplied by Stevens Elastomerics (Northampton, MA). The membrane was washed with water and methanol prior to use in order to remove polar and nonpolar surface contaminants.

Methods

Expression Vector Construction. E. coli genomic DNA was prepared using standard protocols (*29*). *E. coli glpF* DNA was amplified from genomic DNA using the polymerase chain reaction (*30*). The 5′ PCR primer oligonucleotide was identical in sequence to residues 188−217 of the published *glpF* gene (*31*) and its upstream region which encodes a naturally occurring *Bam*HI restriction site. The 3′ primer was complementary to residues 1042−1080 of *glpF* and its downstream region except that an *Xho*I restriction site was incorporated from residues 1069−1074. The amplified DNA was purified by agarose gel electrophoresis, and the 3′ adenine overhangs introduced by *Taq* DNA polymerase were filled in by the Klenow fragment of DNA polymerase I (*32*). DNA termini were phosphorylated with T4 polynucleotide kinase, and the DNA was inserted into the *Sma*I site of pUC18 using T4 DNA ligase. Novablue cells (Novagen) were transformed with pUC18-*glpF* (*33*), and transformants were selected by growth on plates containing LB media (*29*) supplemented with 12.5 μg/mL tetracycline, 25 μg/mL ampicillin, 30 μg/mL 5-bromo-4-chloro-3-indolyl-β-D-galactopyranoside, and 30 μg/mL IPTG. DNA was excised from pUC18 using the *Bam*HI and *Xho*I restriction sites and purified by agarose gel electrophoresis. The DNA was then inserted into a similarly digested pET28b(+) expression plasmid. The pET28b(+) vector (*34*) is designed to incorporate into the expressed protein an amino-terminal His_6 tag for rapid protein purification by immobilized metal affinity chromatography (*35*, *36*), a thrombin cleavage site for removal of the His_6 segment, and an 11 residue T7 epitope for Western immunoblot detection. The expected M_r of the expressed glycerol facilitator including the N-terminal fusion tags is 33 505, and its predicted p*I* is 7.2. BL21(DE3) and BL21(DE3)pLysS cells (*37*) were used as expression hosts. The pLysS-containing cells express small amounts of T7 lysozyme, an inhibitor of T7 RNA polymerase. This can be useful for reducing basal protein expression in the absence of inducer and can improve the viability of cells expressing toxic proteins (*34*, *38*). T7 lysozyme also accelerates cell lysis by hydrolysis of *E. coli* cell wall peptidoglycan, which it can access after the cells have been frozen and thawed. Transformants containing the pET28b(+)-*glpF* construct were selected on LB plates supplemented with the appropriate antibiotic.

DNA Isolation and Sequencing. Plasmid DNA was isolated from 2 mL of *E. coli* cultures using the method developed by Kim and Pallaghy (39). DNA was prepared for sequencing using the modified alkaline lysis method suggested by Perkin-Elmer (http://www.lifesci.ucla.edu/main/dna/ppt.html). *GlpF* DNA was sequenced on an ABI 373A automated sequencer at the University of Calgary Core DNA Services, and a PCR-induced mutation (Asp168Val) was discovered. f1 helper phage R408 (*40*) and the f1 origin of replication on the pET28b(+) vector were used to produce single-stranded plasmid DNA, and the mutation was reverted to

wild type by Kunkel mutagenesis (*41*). The expression vector will be referred to as pET28*glpF*.

Solubilization of Glycerol Facilitator. Sodium dodecyl sulfate (with and without 4 M urea), octyl-β-D-glucopyranoside, *N*-laurylsarcosine, Triton X-100, Tween 80, dodecyl-β-D-maltoside, sodium deoxycholate, and lauryldimethylamine oxide were tested for their ability to extract GF from insoluble *E. coli* cell fractions. Pelleted material was resuspended in buffer A (50 mM sodium phosphate, pH 7.6, 50 mM NaCl, and 10 mM β-mercaptoethanol) plus 1% detergent, and mixed at 4 °C for 1 h. The suspensions were centrifuged, and the supernatants were analyzed for the presence of GF by SDS−PAGE and Western immunoblotting.

Glycerol Facilitator Overexpression and Purification. BL21(DE3)pLysS cells containing pET28*glpF* were grown in antibiotic-supplemented Terrific Broth (*29*) at 37 °C. Glycerol facilitator expression was induced with the addition of 1 mM IPTG when the culture reached an OD_{600} of 0.6−0.7. The bacterial RNA polymerase was arrested by the addition of rifampicin (200 μg/mL) at 1 h following induction, and cells were harvested after a further 1 h of growth (*41*, *42*). The cells were chilled on ice for 5 min and centrifuged at 4000*g* for 10 min. The cell pellets were flash-frozen in liquid nitrogen, defrosted, and resuspended in buffer A. The cells were lysed by passage through 18- and 22-gauge needles. DNA was sheared by sonicating (Fisher Sonic Dismembrator, model 300) the lysed cells on ice 3 times for 30 s. The ruptured cells were then centrifuged at 4 °C for 20 min at 2800*g*. The resulting pellet was resuspended in buffer A containing detergent, and stirred at room temperature for 1 h. The concentrations of the detergents were 3 mM DM, 150 mM SDS, or 150 mM SDS and 4 M urea. Insoluble material was removed by centrifugation, and the supernatant was added to Ni^{2+}-NTA Sepharose preequilibrated in extraction buffer and stirred at room temperature for 1 h. The Sepharose was poured into a column and washed with the extraction buffer. In the case of extraction with urea, prior to elution, the urea was slowly removed using a urea concentration gradient followed by washing with several column volumes of buffer A plus 150 mM SDS at pH 7.6, followed by a second wash at pH 7.2. For the DM and OG preparations, the column was washed in several column volumes of buffer A plus 3 mM DM at pH 6.5. For the OG preparation, the DM was exchanged for OG by washing with buffer A plus 100 mM OG at pH 6.5. Facilitator was then eluted in buffer A plus 150 mM SDS, pH 6.5, or 30 mM DM, pH 4.0, or 100 mM OG, pH 4.0. All samples were analyzed by the SDS−PAGE and Western immunoblotting techniques described below.

Electrophoresis and Immunoblotting. Samples were incubated in 50 mM Tris (pH 6.8), 2% SDS, 0.1% Bromophenol blue, 10% glycerol, and 100 mM DTT for 10 min at 37 °C prior to gel loading. Boiling of GF samples is avoided as this results in protein aggregation to such a degree that a large portion is retained at the interface between the stacking and resolving gels and in the sample well itself (not shown). This is a problem commonly associated with boiling of membrane proteins (*44*). Separation was by SDS−PAGE in Laemmli discontinuous gels (*45*) composed of a 2.5% acrylamide stacking gel and a 10% or 12% resolving gel. After electrophoresis, proteins were visualized either by Coomassie staining or by transfer to a nitrocellulose membrane which was then incubated in a buffer containing anti-T7 antibody−alkaline phosphatase conjugate. Immunoreactive protein was visualized by color development in nitro blue tetrazolium/5-bromo-4-choro-3-indolyl phosphate.

Mass Spectrometry. Purified membrane protein was prepared for mass spectrometry by exchanging SDS for 70 mM octyl-β-D-glucopyranoside by washing Ni^{2+}-NTA-bound GF with a gradient of decreasing concentration of SDS and increasing concentration of OG. GF was eluted from the column as described above. Samples were prepared for MALDI-TOFMS based on protocols developed using polyurethane membrane sample supports (*46*). MALDI-TOFMS was performed in the linear mode on a reflecting time-of-flight mass spectrometer, an instrument built in-house in the Time-of-Flight Lab, University of Manitoba (*47*). An accelerating potential of 25 kV was used. Spectra were obtained using a nitrogen laser (337 nm) (VSL 337 ND, Laser Science Inc., Cambridge, MA) with the fluence adjusted slightly above threshold. To avoid saturation of the detector by low-mass matrix ions, the detector was pulsed on for approximately 19 000 ns after each laser shot. External calibrations for measurements using the PU membrane were performed with protein standards (bovine insulin, equine myoglobin) prepared on similar membrane targets. The spectrum presented here is a summation of approximately 50−100 consecutive shots.

Circular Dichroism Analysis and Deconvolution. All CD experiments were performed on a Jasco-500A CD spectropolarimeter interfaced to a personal computer. The instrument was purged with N_2 at 5 L/min for wavelengths greater than 210 nm and at 25 L/min below 210 nm. For CD experiments, GF was eluted from the Ni^{2+}-NTA column in a 10 mM sodium phosphate buffer containing 10 mM NaCl and detergent (30 mM DM at pH 4.0, or 100 mM OG at pH 4.0, or 150 mM SDS at pH 6.5). Adjustment of the pH was done by adding detergent−buffer solutions at the appropriate pH. Total absorption was always below 1.0 above 200 nm. Samples were placed in a quartz cell with a 0.05 cm path length, and CD spectra were collected at 25 °C, at 2 nm/min between 260 and 205 nm with a time constant of 8 s, and at 0.5 nm/min between 210 and 185 nm with a time constant of 32 s. Baselines were collected in the same fashion on buffer solutions, and spectra were baseline-corrected. The protein concentrations were determined using the calculated molar absorptivity of 38 305 M^{-1} cm^{-1}. Mean residue ellipticities ($[\theta] \times 10^{-3}$ deg·cm²·dmol^{-1}) were calculated using the equation: $[\theta]_M = M\theta/(10)(l)(c)(n)$ where M is 33 505 g/mol, θ is the measured ellipticity in millidegrees, l is 0.05 cm, c is the protein concentration in grams per liter, and $n = 316$ residues. Deconvolution of the CD spectra into pure component spectra was performed using the Convex Constraint Algorithm (CCA) written by Perczel et al. (*50*).

Xylitol Transport Assay. Transport assays were performed as described by Heller et al. (*2*). Briefly, induced and noninduced cells were harvested by centrifugation at 4 °C for 10 min at 2800*g*. A concentrated cell suspension was prepared in buffer A and then diluted into buffer A containing 0 or 250 mM xylitol. Changes in optical density at 600 nm resulting from osmotically induced plasmolysis and deplasmolysis (*49*) were monitored continuously for 5 min.

Chemical Cross-Linking. E. coli membranes were isolated by centrifuging lysed cells at 4 °C for 10 min at 10000*g*. The supernatant was then centrifuged at 4 °C for 1 h at 180000*g*. The resulting pellet, containing crude *E. coli* membranes (*48*), was resuspended in buffer A (minus β-mercaptoethanol) to yield a 10% suspension. For cross-linking, 6 μL of 50 mM disuccinimidyl suberate (DSS) in dimethyl sulfoxide was mixed with 100 μL of a 2% membrane suspension, giving a final concentration of 2.8 mM DSS. Incubations were carried out at 4 °C for various periods of time. The reaction was quenched with the addition of 2.65 μL of 2 mM Tris-HCl, pH 8.0, followed by incubation for 15 min at 4 °C. All samples were analyzed by SDS−PAGE and Western immunoblotting.

RESULTS

Optimization of GF Expression. The *E. coli* expression strain, culture temperature, growth medium, cell density at the point of induction, time of rifampicin addition, and time of harvest after rifampicin addition were varied in order to optimize GF expression. Ten hour growth curves (not shown) indicate that *E. coli* that are overexpressing the glycerol facilitator grow normally after induction with IPTG. A series of experiments in which cells were induced throughout log phase growth (OD_{600} = 0.4−1.4) indicated that the levels of GF expression relative to total cell protein are highest when cells are induced at the mid-log phase of growth and that expression has declined markedly by 4 h following induction, with the optimum harvest time at approximately 2 h. The optimum time for addition of rifampicin was determined to be at 1 h following induction, and GF levels are approximately constant between 1 and 3 h after rifampicin addition. We also found that BL21(DE3)pLysS cells yield slightly more GF than BL21(DE3) cells, and that cells growing in TB medium produce higher yields of GF than those grown in LB medium.

Detergent Solubilization and Purification of GF. Among the eight detergents (see *Materials*) tested, the most effective at extracting glycerol facilitator from *E. coli* are dodecyl-β-D-maltoside, lauryldimethylamine oxide, and sodium dodecyl sulfate, judging from the intensities of the protein bands in Coomassie-stained polyacrylamide gels (data not shown). Octyl glucoside is a poor extraction agent for GF, and SDS/urea is a more effective extraction medium than any of the detergents alone. Lauryldimethylamine oxide promotes extensive protein oligomerization observable in SDS−PAGE and Western immunoblots, and it was not used in any protein purifications.

The extraction of cells with an SDS/urea solution and purification of GF by immobilized-metal affinity chromatography are indicated in the electrophoretogram shown in Figure 1. IPTG stimulates the production of a protein that migrates with an apparent molecular mass of 29 kDa and is most evident in the insoluble cell lysate dissolved in SDS/urea (lane 4). Also apparent in both the Coomassie-stained gel (lane 4) and a Western immunoblot (not shown) is a protein with an apparent mass of 52 kDa. Recombinant protein is not detectable in the noninduced cells (lane 1) or in the soluble fraction of the induced cells (lane 3), and this result was confirmed by Western immunoblotting (not shown). Lane 6 shows that elution of the Ni^{2+}-NTA resin yields protein that electrophoreses at positions corresponding to molecules of mass 29, 52, 75, and 100 kDa. All four recombinant molecules are observable in Western immunoblots of the polyacrylamide gels, suggesting that they are composed of GF oligomers ranging from monomer to tetramer (see below). GF prepared by extraction of cells with SDS/urea never showed aggregates above the tetramer. Neither increasing the dithiothreitol concentration nor adding EDTA (*51*) to the SDS−PAGE sample buffer had any effect on the aggregate distribution (data not shown). Approximately 14.5 mg of 95% pure GF is typically recovered from 9.5 g of cells recovered from 2 L of *E. coli* cell culture.

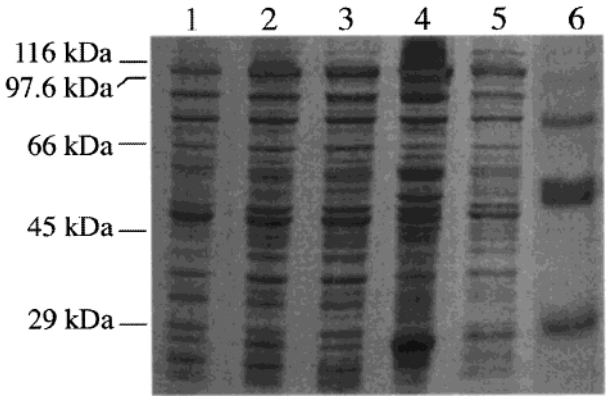

FIGURE 1: Coomassie-stained polyacrylamide gel of SDS/urea-extracted GF purified using a Ni^{2+}-nitrilotriacetic acid column. Lane 1, pre-induction cells; lane 2, post-induction cells; lane 3, soluble cell lysate; lane 4, insoluble cell lysate; lane 5, column flow-through; lane 6, GF eluted from the Ni^{2+}-nitrilotriacetic acid column by lowering the pH. Note the presence of GF monomer, dimer, trimer, and tetramer in lane 6.

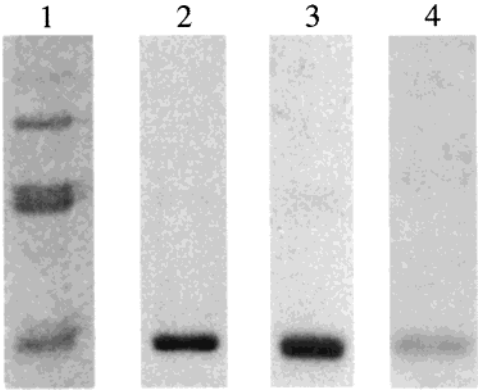

FIGURE 2: Coomassie-stained polyacrylamide gels of glycerol facilitator extracted with: lane 1, SDS/urea; lane 2, SDS; lane 3, DM; lane 4, OG. Monomer, dimer, trimer, and tetramer are visible in the SDS/urea sample.

Figure 2 compares the electrophoretic mobilities of purified recombinant GF dissolved in 150 mM SDS, 30 mM DM, and 100 mM OG. Predominantly monomeric protein is observed in each of the three detergents (lanes 2−4) except when the protein has been extracted with SDS/urea (lane 1). This result is in agreement with the recent work of Lagrée et al. (*52, 53*), who extracted GF from membranes with several detergents and observed only monomeric protein. In contrast, Western immunoblots of the present preparations show that small amounts of oligomeric recombinant protein are present in all the preparations that appear monomeric by Coomassie staining (not shown). Attempts to raise the pH of the OG preparation from 4.0 to 7.6 precipitated the

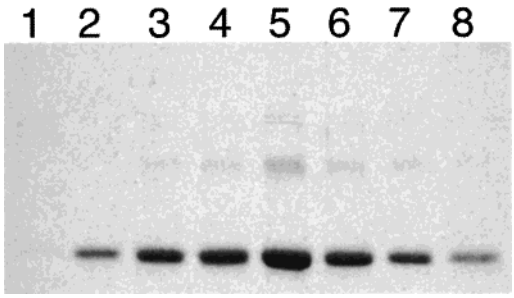

FIGURE 3: Protein concentration dependence of GF oligomer formation. Lane 1, 1.1 μM GF; lane 2, 6.3 μM GF; lane 3, 15 μM GF; lane 4, 19 μM GF; lane 5, 33 μM GF; lane 6, 15 μM GF; lane 7, 7.0 μM GF; lane 8, 4.9 μM GF. DM-purified GF is monomeric at low protein concentrations (lanes 1, 2, and 8), whereas dimer is evident at higher concentrations (lanes 3−7).

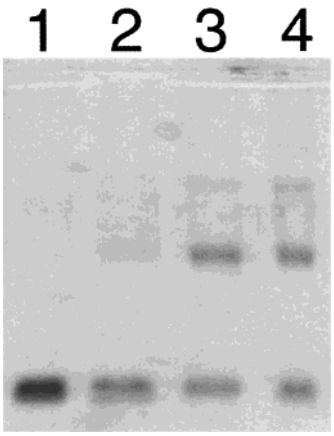

FIGURE 4: Urea-induced aggregation of DM-purified GF. Lane 1, 0 M urea; lane 2, 2 M urea; lane 3, 4 M urea; lane 4, 6 M urea. GF dimer is visible in all samples containing urea; higher molecular weight aggregates are visible at higher urea concentrations in lanes 3 and 4. High molecular weight aggregates appear at the stacking/resolving gel interface in the 6 M urea sample (Lane 4).

protein and produced seven oligomeric species observable in Coomassie-stained SDS−PAGE (not shown). The DM-solubilized protein did not precipitate at pH 7; however, the electrophoretogram in Figure 3 shows that dimeric facilitator (molecular mass 52 kDa) is observable in Coomassie-stained gels in the most concentrated DM-solubilized protein solutions (see lanes 4−6, Figure 3) whereas in dilute solutions the oligomer is not detected in this experiment.

The preparation of proteins for structural analysis by NMR spectroscopy and X-ray diffraction requires highly purified, homogeneous protein preparations. To explore the role of urea in the oligomerization of GF, urea was added at several concentrations to monomeric protein solubilized in 30 mM DM. Figure 4 shows that traces of dimeric GF appear when 2 M urea is present in the DM-solubilized protein solutions (lane 2). At 6 M urea, dimer, trimer, and tetramer are visible in the Coomassie-stained polyacrylamide gels (lane 4), suggesting that urea is promoting oligomerization of the protein.

Mass Spectrometric Analysis of Detergent-Extracted GF. Figure 5 shows the mass spectrum of purified GF obtained from a sample solubilized with 70 mM octyl-β-D-glucopyranoside. A peak corresponding to singly charged GF monomer is present at *m/z* 33 650, and a doubly charged peak is observed at *m/z* 16 841. The observed masses compare well to the theoretical mass of recombinant GF, which is 33 505 Da. No oligomeric species were observed by the mass spectrometer.

Secondary Structure of GF. CD spectra of purified GF were acquired into the far-UV region utilizing the CD optimization parameters of Hennessey and Johnson (*54*). Spectra (Figure 6, solid lines) were collected for the GF dissolved in OG at pH 4.0, DM at pH 4.4 and 7.0, SDS at pH 4.2 and 7.5, and for SDS/urea-extracted protein dissolved in SDS at pH 7.6. In general, the CD spectra display the characteristics of a predominantly α-helical protein with negative bands at 218−222 and 209−212 nm, positive bands at 191−194 nm, and crossover points at 200−203 nm (Figure 6). The ideal α-helical values are 222, 208, 190−195, and 205 nm, respectively (*55*). Convex Constraint Analysis (CCA) (*50, 56*) was used to deconvolute the CD spectra of the glycerol facilitator into their pure structural components (α-helix, β-sheet, β-turn, unordered, and aromatic/disulfide). CCA operates on a data set composed of 24 CD spectra of proteins of known structure and the spectrum of the protein of unknown structure. The results of the deconvolutions of the CD spectra of glycerol facilitator are indicated in Figure 6A,B and are summarized in Table 1. The weighted sums of the pure component spectra (Figure 6, dashed lines) reconstruct the experimental spectra quite well in all cases. The spectra were deconvoluted into three component curves (α-helix, β-sheet, and unordered) except for the spectrum of SDS/urea-extracted protein which required five components to fit the experimental spectrum. In all detergents, the α-helix is the largest secondary structure component. The helix content is highest in DM and SDS (48−55%), is lower in OG (42%), and is lowest in SDS/urea-extracted protein (32%).

Activity of GF in Membranes. The transport properties of the GF have been studied extensively over the last 30 years (*1*−*4, 6, 57, 58*). Heller et al. (*2*) reported that GF will equilibrate a glycerol gradient across the cytoplasmic membrane of *E. coli* within 0.1 min, and stopped-flow techniques have been developed to measure glycerol transport rates indirectly (*4, 57*). GF also facilitates the transport of other low molecular weight polyols, such as xylitol, at a much slower rate. Heller et al. (*2*) reported that xylitol transport is approximately 7 times slower than glycerol transport. Figure 7 illustrates the xylitol transport activity of *E. coli* cells expressing GF and noninduced controls. Both types of cell rapidly plasmolyse when placed in a hypertonic environment. This is observed as a rapid increase in optical density due to light scattering as soon as the cells are placed in the xylitol-containing buffer (■ → ● and ▲ → ◆). Cells induced to express GF (●) have the ability to transport xylitol into the cell and reswell. This is observed as a return of OD_{600} to nearly that of cells in buffer without xylitol (■). Those cells not induced to express GF show no indications of swelling, and remain in a plasmolysed state (◆). We also observe that the addition of mercuric ions (Hg^{2+}) to the cells, prior to the addition of xylitol, blocks transport activity (data not shown) as reported by Maurel et al. (*4*).

Oligomeric State of GF in Membranes. To probe the oligomeric state of membrane-embedded GF, chemical cross-linking was employed using disuccinimidyl suberate. DSS is a lipophilic primary diamine that can penetrate the cell membrane and react with the amino groups of lysines to form a covalent cross-link. Western immunoblots of cell mem-

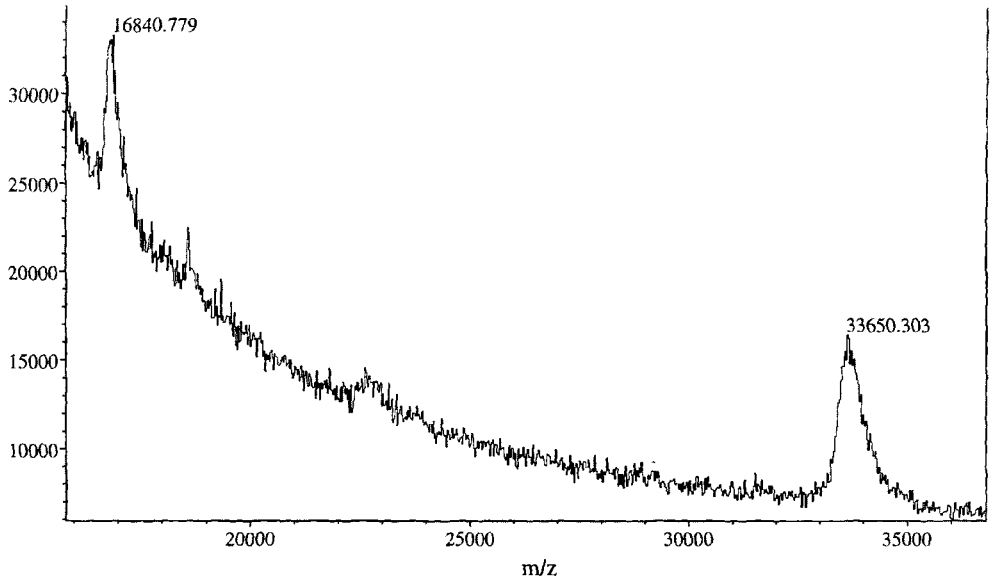

FIGURE 5: MALDI-TOF mass spectrum of detergent-solubilized GF. GF was solubilized in 70 mM octyl-β-D-glucopyranoside (by on-column detergent exchange of SDS), deposited onto a polyurethane membrane, and washed following the protocol developed in (*46*). $[M+H]^+ = 33\,650$ Da (error ~0.4%); the theoretical molecular mass = 33 505 Da. $[M+2H]^{2+} = 16\,841$ Da (error ~0.5%); the theoretical molecular mass = 16 752.5 Da.

brane extracts suggest that the GF exists in membrane predominantly as monomer (Figure 8, lane 1). GF is evidently susceptible to oligomerization in the *E. coli* membrane as the proportion of high M_r protein present in the membrane increases in the presence of cross-linker (Figure 8, lanes 2−4). Furthermore, the species produced by cross-linking are identical in electrophoretic mobility to the species present in the purified, concentrated protein (Figure 1, lane 6). Thus, the facilitator is cross-linked to itself or to another protein of similar mass. Identical results were observed with the cross-linkers disuccinimidyl gluterate, and bis(sulfosuccinimidyl) suberate (data not shown). Cross-linking with DSS for extended periods of time does not produce any observable higher molecular weight species than the apparent tetramer (not shown).

DISCUSSION

One of the impediments to structural analysis of membrane proteins is the small numbers of molecules typically synthesized by cells. A variety of overexpression systems have been explored (*38*), and the one adopted here uses the strong bacteriophage T7 promoter recognized by the T7 RNA polymerase but not by the *E. coli* RNA polymerase. One advantage of this system is that bacterial protein synthesis can be halted with rifampicin, an inhibitor of bacterial RNA polymerase that does not affect the T7 polymerase (*42, 43*). We find that rifampicin increased the yields of GF by over 2-fold. Membrane protein purification is also problematic. The use of polyhistidine segments for protein purification by immobilized metal affinity chromatography has become a widely used practice, and in most cases there is little or no effect of the His segment on protein function or structure (*51, 59*−*61*). Highly pure (Figure 2) glycerol facilitator was prepared using this approach. The xylitol transport activity of recombinant GF (Figure 7) is very similar to that previously reported for native GF (*2, 4, 57*), suggesting that the amino-terminal His_6-T7-tag has little effect on the structure and activity of the recombinant protein which evidently is inserted into the bacterial membrane.

GF Primary and Secondary Structure. MALDI-TOFMS is a powerful analytical tool for accurate mass determination of biomolecules (*62*). However, the presence of ionic detergent and lipid in membrane protein preparations poses a challenge for mass spectrometry. Ionic detergent adducts result in spectra with very low signal-to-noise ratios and poor mass resolution. The use of nonionic detergents, at and above their critical micelle concentrations, has yielded promising results (*63*). We have developed a technique that allows for extensive washing of samples for removal of salts, detergents, and buffers prior to mass spectral analysis (*46*) which increases significantly signal-to-noise ratios and mass resolution compared to unwashed samples. Attempts to remove SDS from GF by this method were unsuccessful; however, exchanging anionic SDS for neutral octyl glucoside on Ni^{2+}-NTA immobilized protein yielded a well-resolved mass spectrum of monomeric GF with adequate signal above the noise. The detergent-exchanged protein, which had been extracted with urea, is oligomeric according to SDS−PAGE; however, MALDI-TOFMS did not detect the oligomeric species. It is possible that the oligomers dissociated in the mass spectrometer or that not enough oligomer was present for detection. We are presently measuring mass spectra on protein purified in OG and DM which did not require exchange of SDS to determine if higher signals and better resolution can be achieved.

Sequence alignments of the *E. coli* GF with the aquaporins (*9*), hydropathy analysis (*17*), and the electron diffraction structures of AQP1 (*23, 24*) suggest that about 47% of the GF is composed of 6 transmembrane α-helices. Electron diffraction data (*64*) also suggest that in aquaporin-1 half of loops B and E fold into short helical segments that form part of the pore of the protein. If the homologous loops are helical in GF, this would elevate the helix content to approximately 55%. CCA analysis (*50*) of the CD spectrum of the glycerol facilitator dissolved in DM indicates that the

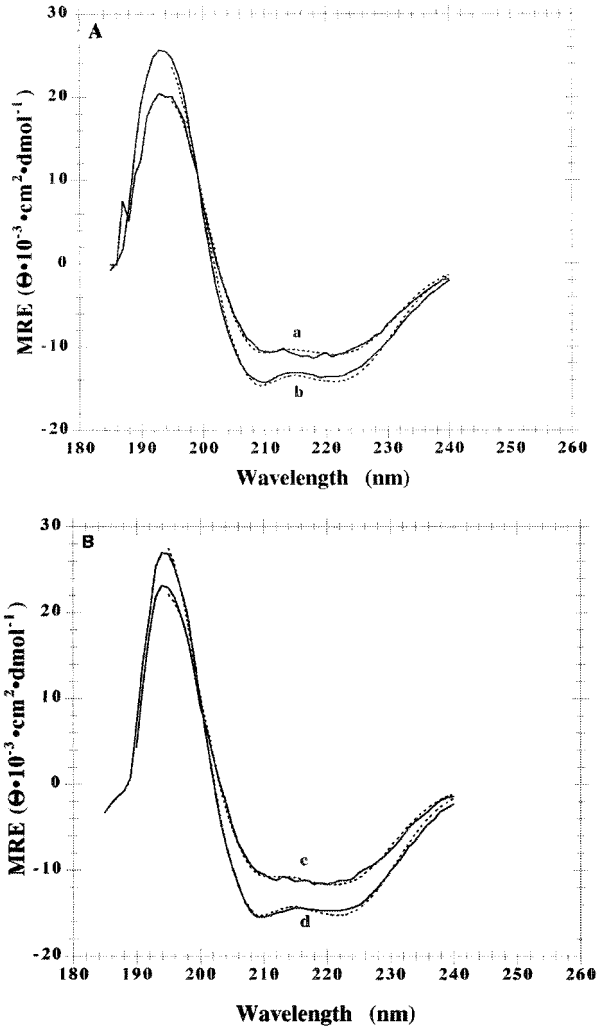

FIGURE 6: CD spectra of GF (solid lines) and fitted spectra from CCA deconvolutions (dotted lines). GF was solubilized in 10 mM sodium phosphate buffer containing 10 mM sodium chloride and detergent at 25 °C. (a) SDS/urea-extracted GF dissolved in SDS at pH 7.6; (b) SDS-extracted GF dissolved in SDS at pH 7.5; (c) DM-extracted GF dissolved in OG at pH 4.0; (d) DM-extracted GF dissolved in DM at pH 4.4. The fitted curves are the weighted sums of the pure components as listed in Table 1.

Table 1: Weights of Pure Structural Components from CCA Deconvolution of the CD Spectra of GF Solubilized in Different Detergent Solutions

	SDS/urea, pH 7.6	SDS, pH 4.2	SDS, pH 7.5	OG, pH 4.0	DM, pH 4.4	DM, pH 7.0
% α-helix	32	48	49	42	55	50
% *β*-sheet	30	30	22	41	22	32
% *β*-turn	18	–	–	–	–	–
% unordered	12	22	29	17	23	18
% aromatic/ disulfide	8	–	–	–	–	–

protein is 50−55% helical (Figure 6 and Table 1), in good agreement with the predictions based on the aquaporin structures. In comparison to SDS, both OG and DM are considered to be nondenaturing detergents. However, OG is a poor extraction agent for the glycerol facilitator, and the protein is prone to precipitation and oligomerization when dissolved in OG. CCA analysis of the CD spectrum indicates that the GF is about 42% α-helical in OG, suggesting that the protein is partially unfolded. The protein appears to be

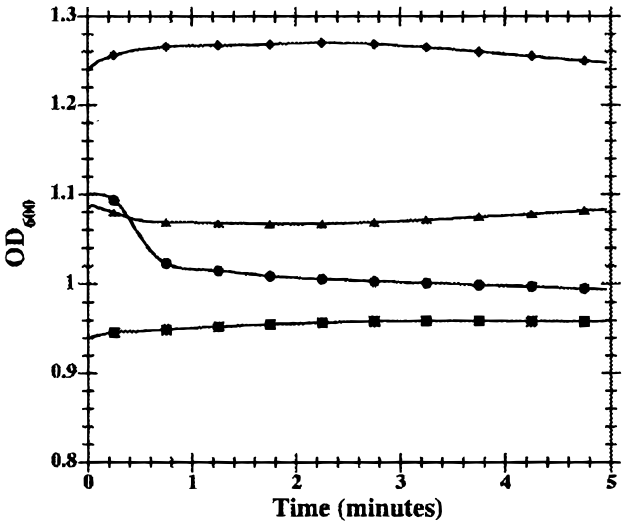

FIGURE 7: Optical changes associated with osmotically induced shrinking and re-swelling of *E. coli* cells. Both induced and noninduced cells plasmolyse rapidly when placed in xylitol-containing buffer. This is observed as an increase in OD_{600} at t = 0 min (■ → ● and ▲ → ◆). Cells diluted in xylitol-free buffer do not shrink [induced (■) and noninduced (▲) cells, respectively]. Only those cells induced to express GF, and therefore transport xylitol, show re-swelling, observable as a decrease in OD_{600} (●).

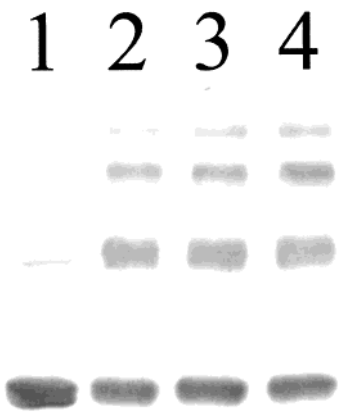

FIGURE 8: Western immunoblot of DSS cross-linked membranes from IPTG-induced *E. coli* cells harboring the pET28*glpF* vector. Lane 1, non-cross-linked membranes; lane 2, membranes cross-linked for 30 min; lane 3, membranes cross-linked for 1 h; lane 4, membranes cross-linked for 2 h.

even more unfolded in SDS when preparation involved extraction from cells in the presence of urea and SDS, because the CD analysis indicates that the facilitator is only 32% helical (Figure 6, Table 1). When urea is omitted from the extraction buffer, the glycerol facilitator exhibits a high helix content (48−49%) in 150 mM SDS. Thus, within the limits of the CD method, SDS does not appear to denature the GF to any greater extent than DM. The CD analysis suggests that portions of the GF are in a nativelike state in both DM and SDS.

Implications of GF Oligomerization. There is considerable evidence that AQP1 (*20, 22*−*24*), AQP4 (*65*), and AQPZ (*48*) exist as tetrameric molecules in membranes. Furthermore, purification and concentration of AQP1 (*19*), AQPZ (*48*), and AQP0 (MIP-26) (*66*) results in the production of oligomers (dimer, trimer, tetramer, and sometimes higher oligomers) observable in SDS−PAGE, suggesting that some aspects of the quaternary structure of these membrane

proteins are retained during electrophoresis. In fact, several other membrane proteins have been demonstrated to partially or completely retain their membranous oligomeric states during SDS−PAGE, including M13 coat protein (*67*), glycophorin A (*68*), the fusion domain of the HIV-1 envelope glycoprotein (gp120−gp41) (*69*), and phospholamban (*70*). Differences in the electrophoretic mobilities of urea-unfolded and detergent-solubilized mitochondrial voltage-dependent anion channel porin on SDS−PAGE strongly suggest that elements of the tertiary structure of this β-barrel membrane protein are preserved during SDS−PAGE. Our observation that the GF has similar helix contents in DM and SDS supports the idea that membrane proteins dissolved in SDS maintain some elements of native structure in SDS including during PAGE. We observe oligomers of GF in SDS−PAGE after the following treatments: heating in SDS, extraction of SDS-solubilized protein with urea/SDS, addition of urea to DM-solubilized protein, preparation of DM-solubilized protein at high concentrations, elevation of the pH in OG-solubilized protein, extraction with LDAO, and chemical cross-linking in membranes. That heating and urea can induce oligomerization suggests that the oligomers represent partially or completely denatured protein, and this is supported by the observation of a lower helix content in the samples with measurable oligomer. On the other hand, dimeric facilitator is observed to form in the absence of any denaturing agents (SDS, urea, heating) when the protein is solubilized with the use of DM and is particularly abundant in concentrated solutions (Figure 3). This suggests the possibility that folded glycerol facilitator monomers have some affinity for self-association. The appearance of putative dimer, trimer, and tetramer within the first 30 min of chemical cross-linking, and the absence of higher molecular weight species suggest that the cross-linking in the membranes is specific (*71*) and support the possibility that the GF can form weakly associated oligomers.

The smaller fraction of glycerol facilitator present as oligomer in SDS−PAGE in comparison to AQPZ (*48*) indicates that the oligomerization of the bacterial facilitator is weaker than that of the bacterial water channel. After entry into the *E. coli* cytoplasm, glycerol is phosphorylated by the glycerol kinase (GK) (*3*). GK shows complex regulatory behavior and is functional in both a dimeric and a tetrameric form (*72*). Fructose 1,6-bisphosphate and the phosphoenolpyruvate phosphotransferase protein IIA^{Glc} are both allosteric inhibitors of GK that bind at different sites (*73*, *74*). Two molecules of fructose 1,6-bisphosphate bind to the GK tetramer, locking it in an inactive tetrameric conformation (*73*), while the phosphocarrier protein IIA^{Glc} binds to each monomer (*75*). There has been considerable speculation and some kinetic evidence that GK exists in close association with GF at the inner membrane and that the kinase may be regulated by interaction with the facilitator (*76*). This has been compared to the interactions of hexokinase and glycerol kinase with the respective mitochondrial porins (*77*). If the facilitator and kinase do interact at the membrane, then changing the oligomeric state of the kinase could influence the oligomeric state of the facilitator and vice versa. Assuming a 1:1 interaction between the two proteins, then both the dimer and tetramer states of GK could have access to glycerol from the associated GF dimer and tetramer, respectively. This would not be possible if GF formed very strong tetramers or if GF could not oligomerize at all, and may explain why GF oligomers are only observed in cross-linking studies or at high protein concentrations. The apparent absence of GF oligomers in *Xenopus* oocyte membranes (*78*) also suggests that oligomerization is weak but raises the possibility that lipid or other components of the *E. coli* membrane may play a role in the activity of the protein as suggested by Truniger and Boos (*7*).

ACKNOWLEDGMENT

We thank Drs. G. Henry and E. Worobec for helpful discussions and Drs. K. Standing and W. Ens for allowing us access to their MALDI-TOFMS instruments.

REFERENCES

1. Lin, E. C. C. (1976) *Annu. Rev. Microbiol. 30*, 535−578.
2. Heller, K. B., Lin, E. C. C., and Wilson, T. H., (1980) *J. Bacteriol. 144*, 274−278.
3. Lin, E. C. C. (1984) Glycerol utilization by facilitated diffusion coupled to phosphorylation in bacteria. in *The cell membrane* (Haber, E., Ed.) pp 109−130, Plenum Publishing Corp., New York.
4. Maurel, C., Reizer, J., Schroeder, J. I., Chrispeels, M. J., and Saier, M. H. (1994) *J. Biol. Chem. 269* (11), 869−872.
5. Calamita, G., Bishai, W. R., Preston, G. M., Giggino, W. B., and Agre, P. (1995) *J. Biol. Chem. 27*0 (29), 63−66.
6. Sanders, O. I., Rensing, C., Kuroda, M., Mitra, B., and Rosen, B., (1997) *J. Bacteriol. 179*, 3365−3367.
7. Truniger, V., and Boos, B. (1993) *Res. Microbiol. 144*, 565−574.
8. Ishibashi, K., Kuwahara, M., Gu, Y., Kageyama, Y., and Tohsaka, A. (1997) *J. Biol. Chem. 272*, 20782−20786.
9. Borgnia, M., Nielson, S., Engel, A., and Agre P. (1999a) *Annu. Rev. Biochem. 68*, 425−458.
10. Tsukaguchi, H., Shayakul, C., Berger, U. V., Mackenzie, B., Devidas, S., Guggino, W. B., van Hoek, A. N., and Hediger, M. A. (1998) *J. Biol. Chem. 273*, 24737−24743.
11. Meinild, A.-K., Klaerke, D. A., and Zeuthen, T. (1998) *J. Biol. Chem. 273*, 32446−32451.
12. Park, J. H., and Saier, M. H. (1996) *J. Membr. Biol. 153*, 171−180.
13. Finkelstein, A. (1987) *Water movement through lipid bilayers, pores, and plasma membranes*, Wiley, New York.
14. Yang, B., and Verkman, A. S. (1997) *J. Biol. Chem. 272*, 16410−16416.
15. Yamamoto, T., and Sasaki, S. (1998) *Kidney Int. 54*, 1041−1051.
16. Gorin, M. B., Yancey, S. B., Cline, J., Revel, J. P., and Horwitz, J. (1984) *Cell 39*, 49−59.
17. Kyte, J., and Doolittle, R. F. (1982) *J. Mol. Biol. 157*, 105−132.
18. Lee, M. D., King, L. S., and Agre, P. (1997) *Medicine 76*, 141−156.
19. Denker, B. M., Smith, B. L., Kuhajda, F. P., and Agre, P. (1988) *J. Biol. Chem. 263*, 15, 634−642.
20. Smith, B. L., and Agre, P. (1991) *J. Biol. Chem. 266*, 6407−6415.
21. Stamer, W. D., Snyder, R. W., and Regan, J. W. (1996) *Biochemistry 35*, (16), 313−318.
22. Verbavatz, J.-M., Brown, D., Sabolic, I., Valenti, G., Ausiello, D. A., Van Hoek, A. N., Ma, T., and Verkman, A. S. (1993) *J. Cell Biol. 123*, 605−618.
23. Walz, T., Hirai, T., Murata, K., Heymann, J. B., Mitsuoka, K., Fujiyoshi, Y., Smith, B. L., Agre, P., and Engel, A., (1997) *Nature 387*, 624−627.
24. Cheng, A., Van Hoek, A. N., Yeager, M., Verkman, A. S., and Mitra, A. K. (1997) *Nature 387*, 627−630.
25. Van Hoek, A. N., Hom, M. L., Luthjens, L. H., de Jong, M. D., Dempster, J. A., and Van Os, C. H. (1991) *J. Biol. Chem. 266*, 16633−16635.

26. Preston, G. M., Jung, J. S., Guggino, W. B., and Agre, P. (1993) *J. Biol. Chem. 26*, 17−20.
27. Jung, J. S., Preston, G. M., Smith, B. L., Guggino, W. B., and Agre, P. (1994) *J. Biol. Chem. 269*, 14648−14654.
28. Preston, G. M., Jung, J. S., Guggino, W. B., and Agre, P. (1994) *J. Biol. Chem. 269*, 1668−1673.
29. Sambrook, J., Fritsch, E. F., and Maniatis, T. (1989) *Molecular cloning: A laboratory manual*, Cold Spring Harbor Laboratory Press, Cold Spring Harbor, NY.
30. Mullis, K., and Faloona, F. (1987) *Methods Enzymol. 155*, 335−350.
31. Muramatsu, S., and Mizuno, T. (1989) *Nucleic Acids Res. 17*, 4378.
32. Clark, J. M. (1988) *Nucleic Acids Res. 16*, 9677−9686.
33. Pope, B., and Kent, H. M. (1996) *Nucleic Acids Res. 24*, 536−537.
34. Studier, F. W., Rosenberg, A. H., Dunn, J. J., and Dubendorff, J. W. (1990) *Methods Enzymol. 185*, 60−89.
35. Hochuli, E., Dobeli, H., and Schacher, A. (1987) *J. Chromatogr. 411*, 177−184.
36. Novagen (1997) *pET system manual*, 7th ed.
37. Studier, F. W., and Moffatt, B. A. (1986) *J. Mol. Biol. 189*, 113−130.
38. Grisshammer, R., and Tate, C. G. (1995) *Q. Rev. Biophys. 28*, 315−422.
39. Kim, K.-S., and Pallaghy, C. K. (1996) U.S. Department of Commerce/NOAA/NMFS/NWFSC/Molecular Biology Protocols (http://research.nwfsc.noaa.gov/protocols/dna-prep.html.).
40. Russel, M., Kidd, S., and Kelley, M. R., (1986) *Gene 45*, 333−338.
41. Kunkel, T. A., Bebenek, K., and McClary, J. (1991) *Methods Enzymol. 204*, 125−139.
42. Kurucz, I., Jost, C. R., George, A. J., Andrew, S. M., and Segal, D. M. (1993) *Proc. Natl. Acad. Sci. U.S.A. 90*, 3830−3834.
43. Kuderova, A., Nanak, E., Truksa, M., and Brzobohaty, B. (1999) *Protein Express. Purif. 16*, 405−409.
44. Sagne, C., Isambert, M.-F., Henry, J.-P., and Gasnier, B. (1996) *Biochem. J. 316*, 825−831.
45. Laemmli, U. K. (1970) *Nature 227*, 680−685.
46. McComb, M. E., Oleschuk, R. D., Manley, D. M., Donald, L., Chow, A., O'Neil, J. D., Duckworth, H. W., Ens, W., Standing, K. G., Perreault, H., (1997) *Rapid. Commun. Mass Spectrom. 11*, 1716−1722.
47. Tang, X., Beavis, R. C., Ens, W., Lafortune, F., Schueler, B., and Standing, K. G. (1988) *Int. J. Mass Spectrom. Ion Proc. 85*, 43−49.
48. Borgnia, M. J., Kozono, D., Calamita, G., Maloney, P. C., and Agre P. (1999b) *J. Mol. Biol. 291*, 1169−1179.
49. Latimer, P. (1982) *Annu. Rev. Biophys. Bioeng. 11*, 129−150.
50. Perczel, A., Hollósi, M., Tusnady, G., and Fasman, G. D. (1991) *Protein Eng. 4*, 669−679.
51. Hom, L. G., and Volkman, L. E. (1998) *BioTechniques 25*, 20−22.
52. Lagrée, V., Froger, A., Deschamps, S., Isabelle, P., Delamarche, C., Bonnec, G., Gouranton, J., Thomas, D., and Hubert, J.-H. (1998) *J. Biol. Chem. 273*, 33949−33953.
53. Lagrée, V., Froger, A., Deschamps, S., Hubert, J.-F., Delamarche, C., Bonnec, G., Thomas, D., Gouranton, J., and Pellerin, I. (1999) *J. Biol. Chem. 274*, 6817−6819.
54. Hennessey, J. P., Jr., and Johnson, W. C., Jr. (1982) *Anal. Biochem. 125*, 177−188.
55. Fasman, G. D. (1993) *Biotechnol. Appl. Biochem. 18*, 111−138.
56. Perczel, A., Park, K., and Fasman, G. D. (1992) *Anal. Biochem. 203*, 83−93.
57. Alemmohamad, M. M., and Knowles, C. J. (1974) *J. Gen. Microbiol. 82*, 125−142.
58. Hayashi, S.-I., and Lin, E. C. C. (1965) *Biochim. Biophys. Acta 94*, 479−487.
59. Knol, J., Veenhoff, L., Liang, W.-J., Henderson, P. J. F., Leblanc, G., and Poolman, B. (1996) *J. Biol. Chem. 271*, 15358−15366.
60. Patzlaff, J. S., Moeller, J. A., Barry, B. A., and Brooker, R. J. (1998) *Biochemistry 37*, 15363−15375.
61. Pourcher, T., Leclercq, S., Brandolin, G., and Leblanc, G. (1995) *Biochemistry 34*, 4412−4420.
62. Amado, F. M. L., Santana-Marques, M. G., Ferrer-Corria, A. J., and Tomer, K. B. (1997) *Anal. Chem. 69*, 1102−1106.
63. Rosinke, B., Strupat, K., Hillenkamp, F., Rosenbusch, J., Dencher, N., Krüger, U., and Galla, H.-J. (1995) *J. Mass Specrom. 30*, 1462−1468.
64. Mitsouka, K., Murata, K., Walz, T., Hirai, T., Agre, P., Heymann, J. B., Engel, A., and Fujiyoshi, Y. (1999) *J. Struct. Biol. 128*, 34−43.
65. Neeley, J. D., Christensen, B. M., Nielsen, S., and Agre, P. (1999) *Biochemistry 38*, 11156−11163.
66. Horwitz, J., and Bok, D. (1987) *Biochemistry 26*, 8092−8098.
67. Li, Z., and Deber, C. M. (1991) *Biochem. Biophys. Res. Commun. 180*, 687−693.
68. Mingarro, I., Whitley, P., Lemmon, M. A., and Heijne, G. V. (1996) *Protein Sci. 5*, 1339−1341.
69. Prikster, M., Rucker, J., Hoffman, T. L., Doms, R. W., and Shai, Y. (1999) *Biochemistry 38*, 11359−11371.
70. Adams, P. D., Engelman, D. M., and Brünger, A. T. (1996) *Proteins: Struct., Funct., Genet. 26*, 257−261.
71. Ji, T. H., and Middaugh, C. R. (1980) *Biochim. Biophys. Acta 603*, 371−374.
72. De Riel, J. K., and Paulus, H. (1978) *Biochemistry 17*, 5141−5145.
73. Ormo, M., Bystom, C. E., and Remington, S. J. (1998) *Biochemistry 37*, 16565−16572.
74. Bystrom, C. E., Pettigrew, D. W., Branchaud, B. P., O'Brien, P., and Remington, S. J. (1999) *Biochemistry 38*, 3508−3518.
75. Hurley, J. H., Faber, H. R., Worthylake, D., Meadow, N. D., Roseman, S., Pettigrew, D., and Remington, S. J. (1993) *Science 259*, 673−677.
76. Voegele, R. T., Sweet, G. D., and Boos, W. (1993) *J. Bacteriol. 175*, 1087−1094.
77. Brdiczka, D. (1990) *Experientia 46*, 161−167.
78. Bron, P., Lagree, V., Froger, A., Rolland, J.-P., Hubert, J.-F., Delamarche, C., Deschamps, S., Pellerin, I., Thomas, D., and Haase, W. (1999) *J. Struct. Biol. 128*, 287−296.

BI000703T